Ecotoxicology and Environmental Safety 133 (2016) 164–175

Contents lists available at ScienceDirect

Ecotoxicology and Environmental Safety

journal homepage: www.elsevier.com/locate/ecoenv

Indoor radon risk associated to post-tectonic biotite granites from Vila Pouca de Aguiar pluton, northern Portugal

L.M.O. Martins [a,*], M.E.P. Gomes [a], R.J.S. Teixeira [a], A.J.S.C. Pereira [b], L.J.P.F. Neves [b]

[a] CEMUC, Department of Geology, University of Trás-os-Montes e Alto Douro, Quinta de Prados, 5000-801 Vila Real, Portugal
[b] CEMUC, Department of Earth Sciences, University of Coimbra, 3000-272 Coimbra, Portugal

ARTICLE INFO

Article history:
Received 3 December 2015
Received in revised form
13 May 2016
Accepted 11 July 2016
Available online 22 July 2016

Keywords:
Indoor radon
Effective dose
Radionuclides
Granites
Dwellings

ABSTRACT

At Vila Pouca de Aguiar area, northern Portugal, crops out a post-tectonic Variscan granite pluton, related with the Régua-Vila Real-Verín fault zone, comprising three types of biotite granites. Among these granites, PSG granite yield the highest average contents of U, probably due to its enrichment in accessory U-bearing minerals such as zircon. In the proximity of faults and joints, these granites are often affected by different degrees of hydrothermal alteration, forming reddish altered rocks, commonly known as "episyenites". These altered rocks are probably associated to the occurrence of hydrothermal processes, which led to uranium enrichment in the most advanced stages of episyenitization. In these granites, both average gamma absorbed dose rates in outdoor and indoor air are higher than those of the world average. Furthermore, even in the worst usage scenario, all these granites can be used as a building material, since their annual effective doses are similar to the limit defined by the European Commission. The geometric mean of radon activity of 91 dwellings located at the Vila Pouca de Aguiar pluton is 568 Bq m^{-3}, exceeding that of other northern Portuguese granites. Measurements carried out during a winter season, indicate that 62.6% of the analysed dwellings yield higher indoor radon average values than the Portuguese legislation limit (400 Bq m^{-3}), and annual effective doses due higher than the world's average value (1.2 mSv y^{-1}).

The interaction of geogenic, architectural and anthropogenic features is crucial to explain the variance in the geometric mean of radon activity of dwellings from Vila Pouca de Aguiar pluton, but the role of geologic faults is probably the most important decisive factor to increase the indoor radon concentration in dwellings. Hence, the development of awareness campaigns in order to inform population about the incurred radiological risks to radon exposure are highly recommended for this specific area.

1. Introduction

Radon is a noble radioactive gas, resulting from uranium decay and characterised by a high mobility in natural systems. Exposure to this gas can be a serious public health problem, since it is responsible for approximately half of the radiation dose received by the human population (UNSCEAR, 2008). According to the Environmental Protection Agency radon gas is reported as the second leading risk factor of lung cancer after tobacco, which is in accordance to recent epidemiological studies carried out in the European Union, suggesting that radon inside dwellings may cause about 20,000 deaths per year (Dubois, 2005). The risk rises 16% for every 100 Bq m^{-3} increase in residential concentrations (Darby et al., 2005). Lung cancer mortality in northern Portugal was assessed by Veloso et al. (2012), using data provided by the North Regional Health Administration and indoor radon concentrations from a national survey conducted by the Portuguese Environmental Agency. A sub multiplicative interaction between smoking and indoor radon exposure was considered for the estimation of the number of lung cancer deaths attributed to indoor radon exposure, which ranges from 1565 to 2406, for the period between 1995 and 2004. This study indicated that among the 8514 lung cancer deaths observed, from 18 to 28% could be associated with indoor radon exposure.

The main source of indoor radon are the radionuclides in the underlying soils and rocks, which can diffuse into indoor air, but in some cases building materials can also contribute for radon exposure (Janik et al., 2015). Indoor radon could be controlled by a large number of geogenic, climatic and anthropogenic factors, which must be studied and monitored in order to access the health risk (Cosma et al., 2013, 2015). Among geogenic factors, the local structural geology assumes a primordial role in the prediction of indoor radon concentrations and radiometric anomalies associated with faults, as it is demonstrated by Pereira et al. (2010) in Central Portugal and Drolet and Martel (2016) in the Province of Quebec,

* Corresponding author.
E-mail address: lisa_martins@hotmail.com (L.M.O. Martins).

http://dx.doi.org/10.1016/j.ecoenv.2016.07.009
0147-6513/

Canada. However, many other studies put in evidence the relationship between Rn and uranium-rich granitic sources, such as those carried out by Bossew et al. (2008) in Austria, Ielsch et al. (2010) in the region of Bourgogne, Massif Central, France, Kemski et al. (2009) in the Fichtelgebirge and Erzgebirge areas, Germany, Appleton and Miles (2010) in England and Cho et al. (2015) in South Korea.

Several studies proved that the relation between indoor radon and climate is complex and, in many situations, inconclusive (e.g. Kobayashi, 2000; Miles, 2001; Groves-Kirkby et al., 2006). In fact, Groves-Kirkby et al. (2015) indicate that, in the town of Northampton, England, the monthly arithmetic mean radon concentration shows minimal or zero cross-correlation with temperature, atmospheric pressure and wind-speed, but there is a minimal negative correlation with precipitation and possibly also with relative humidity. The same study demonstrates that there are evidences of significant latency response in radon concentrations in respect to some climatic parameters, especially those related with the presence of atmospheric moisture. On the other hand, Perrier et al. (2009) and Perrier and Girault (2013) have demonstrated the sensitivity of soil-gas radon concentration to atmospheric pressure changes. The anthropogenic influences and the architectural characteristics of the structures (building age, floor level, foundation, building material, building type, room type) could also be important to explain the distribution of indoor radon concentrations (e.g. Kemski et al., 2009; Friedmann and Groeller, 2010; Girault and Perrier, 2012; Kropat et al., 2014).

In this context, it is extremely important to understand, in a first stage, the influence of the geology in the indoor radon variation, and, whenever necessary, to inform the population about the incurred radiological risks if no preventive measures were taken (Appleton et al., 2011). The Portuguese legislation regarding the air quality allows radon concentrations up to 400 Bq m^{-3} inside of dwellings, and the measurement of this gas is only required in new constructions within granitic areas (Decree-Law nr. 79/2006). In Portugal, indoor radon exposure has been largely ignored, as in many other countries, by government or health authorities. Worldwide annual exposure to natural radiation sources ranges from 1 to 10 mSv y^{-1}, being its average estimated in 2.4 mSv y^{-1}. About 1.2 mSv y^{-1} is due to the exposure of radon inhalation (UNSCEAR, 2000).

The present study systematises radiometric and indoor radon results gathered at the Vila Pouca de Aguiar pluton (northern Portugal) to assess the indoor radon risk in dwellings located in an area with an important regional fault system intersecting different granitic rocks. These ones show different degrees of alteration (episyenitization) and weathering. This work also intended to evaluate the influence of house configuration and indoor human behaviour patterns in the radon gas exposure.

2. Geological setting

At Vila Pouca de Aguiar area, northern Portugal, crops out a post-tectonic Variscan granite pluton, with ca. 200 km^2 and an elongated form, constrained by NNE-SSW fractures related with the Régua-Vila Real-Verín fault zone (Fig. 1a and b). The post-tectonic granite pluton comprises three types of biotite granites: Telões granite (TLG), Pedras Salgadas granite (PSG) and Souto granite (STG) that are variably porphyritic (Fig. 1b). Scarce rounded microgranular mafic enclaves of granodioritic and, more rarely, tonalitic composition, varying in size from 10 to 20 cm, are also observed especially in the TLG (Gomes, 2008). Souto granite is a coarse grained rock, outcropping in a small area in the south, southwest and east of the pluton. The three granites can be distinguished macroscopically by their grain size and biotite content, but there are no clear-cut contacts between the two dominant granites (TLG and PSG). The Vila Pouca de Aguiar granite pluton cross-cuts two-mica syntectonic granites, related to the third deformation phase (D_3) of the Variscan event, as well as the Upper Ordovician to Lower Devonian metasedimentary sequence (Ribeiro, 1998; Martins et al., 2009), developing a metamorphic contact aureole. Based on geological, geochemical, isotopic, AMS and gravity data, Sant'Ovaia et al. (2000) and Martins et al. (2009) determined that the Vila Pouca de Aguiar granite pluton is a normally zoned composite laccolith, yielding older, more mafic marginal phases toward younger, more felsic central phases, that has been emplaced at the very end of the Variscan orogeny, fed by magma that upwelled from the fault zone. Its zoning is related to the successive emplacement of two main independent magma batches. The emplacement of this pluton was strongly constrained by the Régua-Vila Real-Verín fault zone, which crosscuts whole northern Portugal. This fault system began its development during the deformation phase D_3 of the Variscan orogeny, being reactivated on the deformation phase D_4 as a sinistral strike-slip fault with transtensional component. After that, with the rotation of the main stress direction to E-W, the Régua-Vila Real-Verín fault zone was reactivated as a thrust fault (Baptista, 1998). At present, this fault zone still has seismic activity (Fig. 1a and b) (Baptista, 1998).

At Vila Pouca de Aguiar pluton, granites are affected by various stages and degrees of weathering, increasing with the proximity of faults and joints. On the other hand, the occurrence of reddish altered rocks, commonly known as “episyenites”, is constrained to TLG and PSG granites. These episyenites probably resulted from a hydrothermal alteration process and involved alkali metasomatism, magmatic quartz dissolution and transformation of the granite primary minerals (Genter and Traineau, 1992; Genter et al., 2002; Dezayes et al., 2005; Jaques et al., 2010). Two degrees of alteration can be distinguished: a) pervasive rock mass alteration, affecting large areas of the granite without visible modification of the rock texture and b) vein alteration, where the primary minerals (silicates) of the granite have been partly dissolved.

Due to the abundance of granites in the studied region, these rocks are frequently employed as building material by the locals, namely in the form of blocks in dwelling walls or as small slabs and tiles for lining purposes in external walls. Granites are also commonly used in indoor paving, kitchen counters, fireplaces and as coarse aggregates in the production of concrete.

3. Material and methods

The petrographic study of polished thin sections of non-altered and episyenitized granites was carried out at the Department of Geology of University of Trás-os-Montes e Alto Douro, whereas backscattered electron imaging was performed at the National Laboratory of Energy and Geology (LNEG), S. Mamede de Infesta, Portugal.

A portable GF Instruments γ-ray spectrometer, model Gamma Surveyor compact 2, equipped with a NaI detector and a measuring range of 100 Kev to 3 MeV was employed in the field radiometric survey, covering different granite areas and the associated episyenitized domains, with a total of 84 analysis. Besides the gamma-ray flux, this technique also allows the estimation of K, eU and eTh concentrations. In each site the spectrometer was set close to the rock surface and then three measurements were made during a period of two minutes each. The final value resulted from the average of those three measurements.

Based on the field radiometric survey, 15 representative samples were selected for precise radiometric laboratory measurements, using a high efficiency multichannel gamma-ray spectrometer (ORTEC), equipped with a 3″ NaI (Tl) crystal detector and Digibase system. The detection limit for K, U and Th are 0.1%,

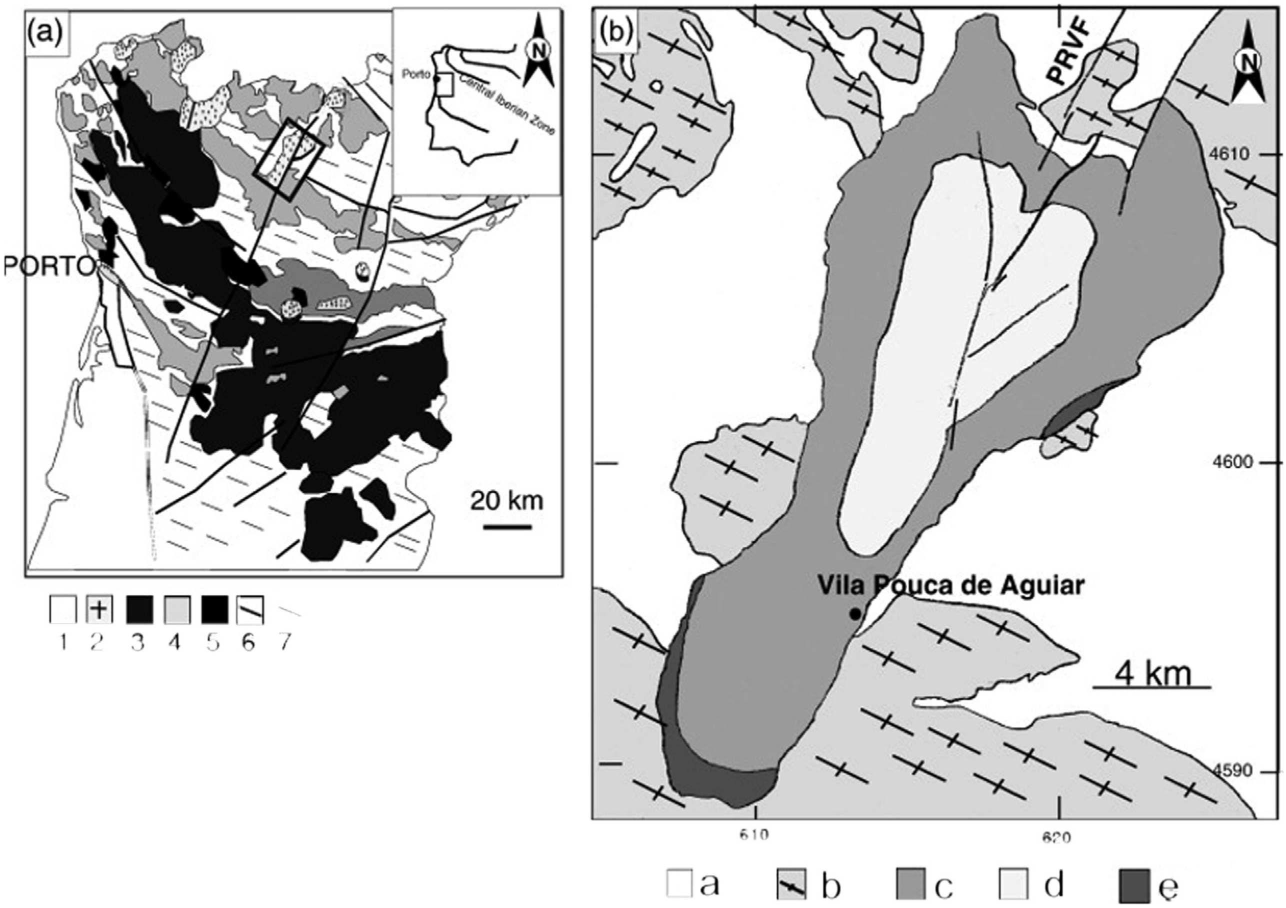

Fig. 1. (a) Geological distribution of Variscan syn to post-orogenic granitoids in Central Iberian Zone. 1. Post Palaeozoic; 2. Post-orogenic biotite granites; 3. Late-orogenic biotite granites; 4. Synorogenic two-mica granites; 5. Synorogenic biotite granites; 6. Metasedimentary rocks; 7. Faults. (b) Sketch maps of the Vila Pouca de Aguiar plutons. a. Metasedimentary rocks; b. Syntectonic two-mica granite; c. Telões granite (TLG); d. Pedras Salgadas granite (PSG); e. Souto granite (STG). Coordinates: UTM kilometric system; PRVF: Penacova-Régua-Verin Fault; (modified from Martins et al., 2009)
.

0.5 and 1 ppm, respectively. These measurements were carried out at the Natural Radioactivity Laboratory, University of Coimbra (LRN). Each sample was crushed to about 2 mm size and well mixed to ensure homogeneity in minerals distribution. The prepared samples, weighing between from 300 to 500 g, were placed in a standard-size plastic container (Marinelli beakers). The sample containers were sealed to prevent as much as possible any gas escape and left undisturbed for a minimum period of four weeks, in order to achieve isotopic equilibrium in the decay chains of U and Th. After this period, each sample was measured and the signals were acquired during 10 h. The resulting spectrum was analysed with the software Scintivision32 © to quantify ^{40}K, ^{214}Bi and ^{208}Tl peaks. Assuming secular equilibrium, K_2O concentration was estimated from ^{40}K activity (1460 keV), U from ^{214}Bi (1760 keV) and Th from ^{208}Tl (2614 keV). Background subtraction was performed for each measurement (Lamas et al., 2015). This system was previously implemented and calibrated in the LRN, with standards certified by the International Atomic Energy Agency (IAEA).

Field studies also included a standard measurement of gamma absorbed dose rate at a height of 1 m above the ground for 2 min. A long counting time was used to minimise variability. Some measurements were also carried out inside dwellings.

The annual effective dose equivalent (*AEDE*) was calculated according to UNSCEAR (2000) as:

$$AEDE\left(\mu Sv\ y^{-1}\right) = D \times DCF \times OF \times T \tag{1}$$

where *D* is absorbed dose rate in air (ηGy h^{-1}), *DCF* is a dose conversion factor (0.7 SvG y^{-1}), *OF* is the outdoor occupancy factor equal to 0.2 and *T* is time factor (8.760 h y^{-1}).

Using absorbed doses measurements, annual effective dose from population's exposure to gamma radiation background (*E*) was estimated from UNSCEAR (2000) as follow:

$$E\left(mSv\ y^{-1}\right) = \left(D\ out \times OF\ out + D\ in \times OF\ in\right) \times T \times CC/\ 1000000 \tag{2}$$

where *D out* and *D in* (ηGy h^{-1}) are mean outdoor and indoor absorbed dose rates, *T* (hours) is a time conversion factor (8760 h), *OF out* and *OF in* are outdoor and indoor occupancy factors (20% and 80% for outdoor and indoor, respectively) and *CC* is the conversion coefficient (0.7 for adults) reported by UNSCEAR (2000) to convert absorbed dose in air to the effective dose in humans.

Indoor radon concentrations were determined using CR-39 passive detectors in 91 dwellings built on different lithologies, during the winter season. Among the studied dwellings, 23% were mainly built with local granites, 28% with local granites and light-weight clay bricks and 49% with light-weight clay bricks. Detectors were placed in the ground floors and/or first floors of dwellings, and the period of exposure was about three months, between December 2013 and March 2014. During the winter period, dwellings are less ventilated and consequently the radon concentration is generally higher than summer period. After the exposure period time, the CR-39 passive detectors were chemically etched during 4 h in a NaOH solution, at a temperature of 90 ºC, in the LRN. Track density to radon activity conversion factors are provided by the manufacturer for each batch of detectors, following specific exposures in radon certified calibration chambers (Lamas et al., 2015). The annual effective dose (H) for inhabitants of the studied region was calculated from the determined value of indoor radon concentration (CRn), using the equation given by UNSCEAR (2000):

$$H\left(mSv\ y^{-1}\right) = CRn \times F \times O \times DCF \tag{3}$$

where F is the global average of equilibrium factor for radon and its progeny (0.4), O is the global average indoor occupancy factor (7000 h y^{-1}) and DCF is the dose conversion factor (9 ηSv h^{-1}(Bq m^{-3})$^{-1}$) for radon and its progeny.

4. Results and discussion

4.1. Petrography and accessory minerals in granites

The studied rocks correspond to monzogranites, which contain 30–32% modal quartz, 20–24% perthitic K-feldspar (orthoclase and microcline) and 37–42% normally zoned plagioclase with oligoclase-andesine composition in the TLG and a albite-oligoclase composition in the PSG and STG. Biotite, with a modal average of 9% in TLG and 5% in PSG and STG, is the only ferromagnesian phase (Martins et al., 2009). Muscovite reach up to 1% in PSG and STG. Petrographic and electron microprobe studies indicate the presence of U- and Th-bearing accessory minerals, especially zircon and allanite in TLG (Fig. 2a), monazite, xenotime and zircon in PSG (Fig. 2b) and STG (Fig. 2c), including thorite in the latter (Fig. 2c and d). Apatite occurs in all studied granites as large crystals (Fig. 2d), usually containing inclusions of zircon, monazite and ilmenite. Locally, apatite also occurs as clear acicular crystals. Zircon and monazite are abundant, sometimes as euhedral crystals, included, in biotite and apatite. Allanite is also frequent and occurs as large zoned crystals. Xenotime occurs associated to zircon. Thorite has been found included in allanite and apatite cracks. These accessory minerals were also identified by Gomes (2008) in TLG that also reported the presence of titanite.

4.2. Potassium, uranium and thorium contents and indoor radon risk

The average contents of K in non altered TLG, PSG, STG and in the episyenitized stages of TLG and PSG (TLEPG and PSEPG) range, respectively, from 4.61% to 6.58%, from 9.67% to 18.47% and from 24.84% to 28.34% (Fig. 3a–c; Appendix A). Among all granites, the TLEPG yield the highest average contents of K and eU, whereas the STG shows the lowest average contents of K and eU (Fig. 3a and b). According to Martins et al. (2009), the potassium, uranium and thorium contents measured in granites TLG and PSG of Vila Pouca de Aguiar pluton are always higher than the crustal average (K- 2.1%, U- 2.7 ppm and Th- 9.6 ppm).

The laboratory measurements, using a multichannel gamma-ray spectrometer (ORTEC), equipped with a lead shield, support those achieved with the portable GF Instruments γ-ray spectrometer (Fig. 3d–f). However, the laboratory data evidenced some radiometric anomalies, in particular the U enrichment of PSEPG, corresponding to the highest detected average with 36 ppm (Fig. 3e). The laboratory measurements also have shown that, among non-altered granites, the PSG yields the highest average contents of U, whereas STG shows the highest average contents of Th (Fig. 3f). The PSG enrichment in U is most probably due to the ubiquitous presence of zircon, whereas the Th enrichment of STG is mainly related to the presence of thorite and also monazite and

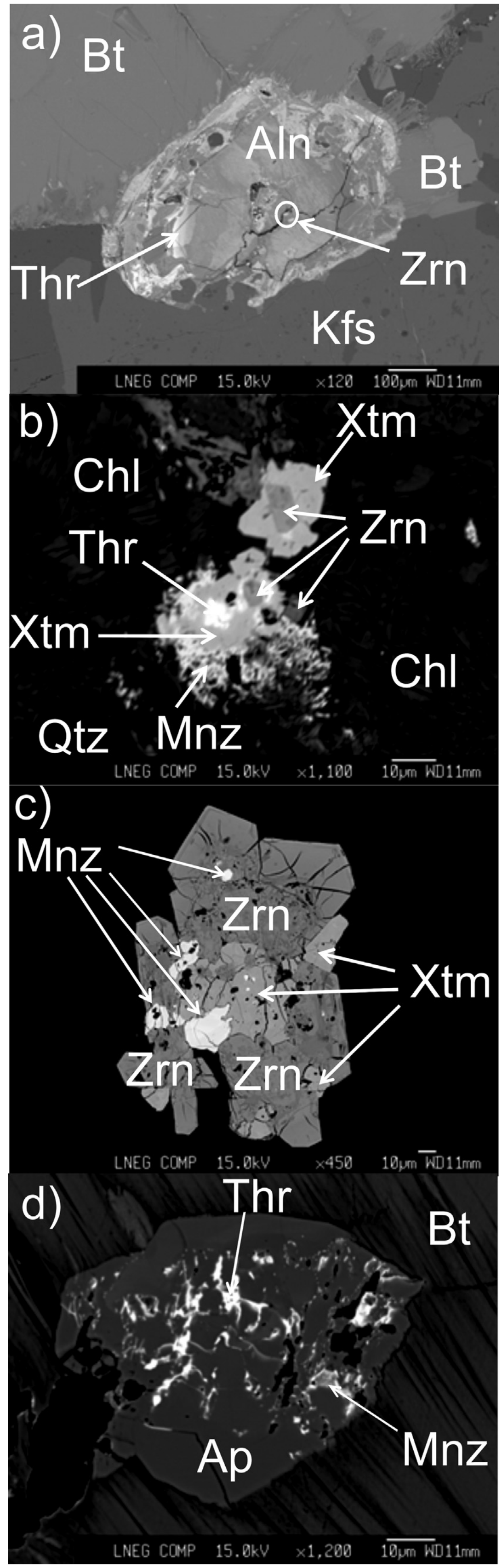

Fig. 2. Backscattered electron images of accessory minerals: a) allanite (Aln), zircon (Zrc), thorite (Thr), biotite (Bt) and potassium feldspar (Kfs) in TLG; b) xenotime (Xtm), zircon (Zrc), monazite (Mnz), quartz (Qz) and chlorite (Chl) in PSG; c) xenotime (Xtm), zircon (Zrc) and monazite (Mnz) in STG; d) biotite (Bt) and apatite (Ap) containing monazite (Mnz) and thorite (Thr) inclusions in STG.

Please cite this article as: Martins, L.M.O., et al., Indoor radon risk associated to post-tectonic biotite granites from Vila Pouca de Aguiar pluton, northern Portugal. Ecotoxicol. Environ. Saf. (2016), http://dx.doi.org/10.1016/j.ecoenv.2016.07.009

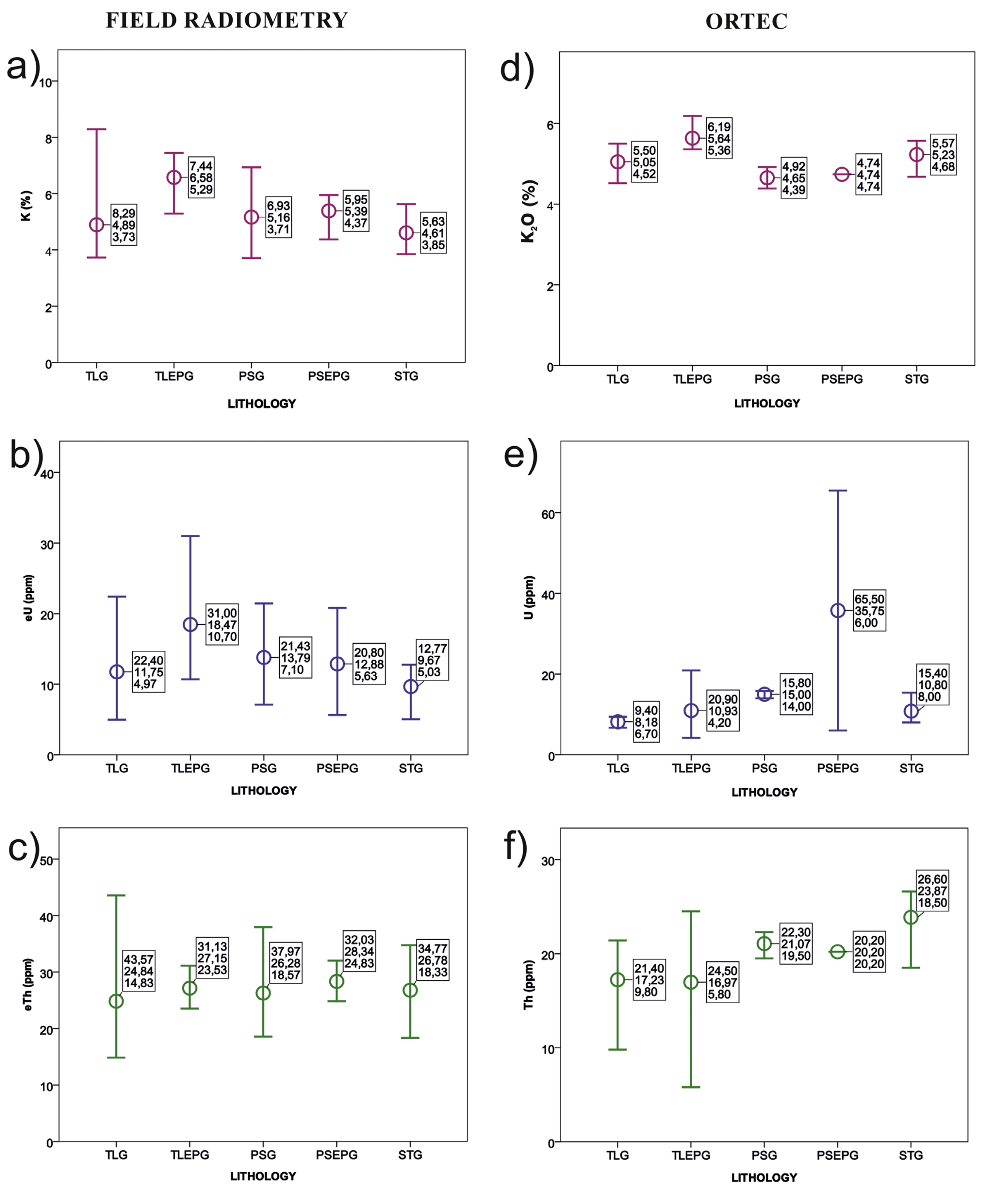

Fig. 3. High-low diagrams with average, minimum and maximum concentrations of radiometric field values: a) K, b) eU and c) eTh and concentrations of: d) K_2O, e) U and f) Th using laboratory ORTEC in outcropping rocks from Vila Pouca de Aguiar pluton.

xenotime. The eU content of PSG is above 14 ppm and, therefore, comparable to those from uraniferous granites (Wilson and Åkerblom, 1982; Cambon, 1994; Basson and Greenway, 2004; Appendix B). The relation between eU and eTh in the studied granitic rocks do not show a positive correlation (Fig. 4a), indicating that the distribution of both uranium and thorium is no longer due to magmatic process, such as fractional crystallisation (Charbonneau, 1982; Heikal et al., 2013). Taking into account that uranium is very susceptible to transportation/leaching processes under post-magmatic/late hydrothermal and weathering

Please cite this article as: Martins, L.M.O., et al., Indoor radon risk associated to post-tectonic biotite granites from Vila Pouca de Aguiar pluton, northern Portugal. Ecotoxicol. Environ. Saf. (2016), http://dx.doi.org/10.1016/j.ecoenv.2016.07.009

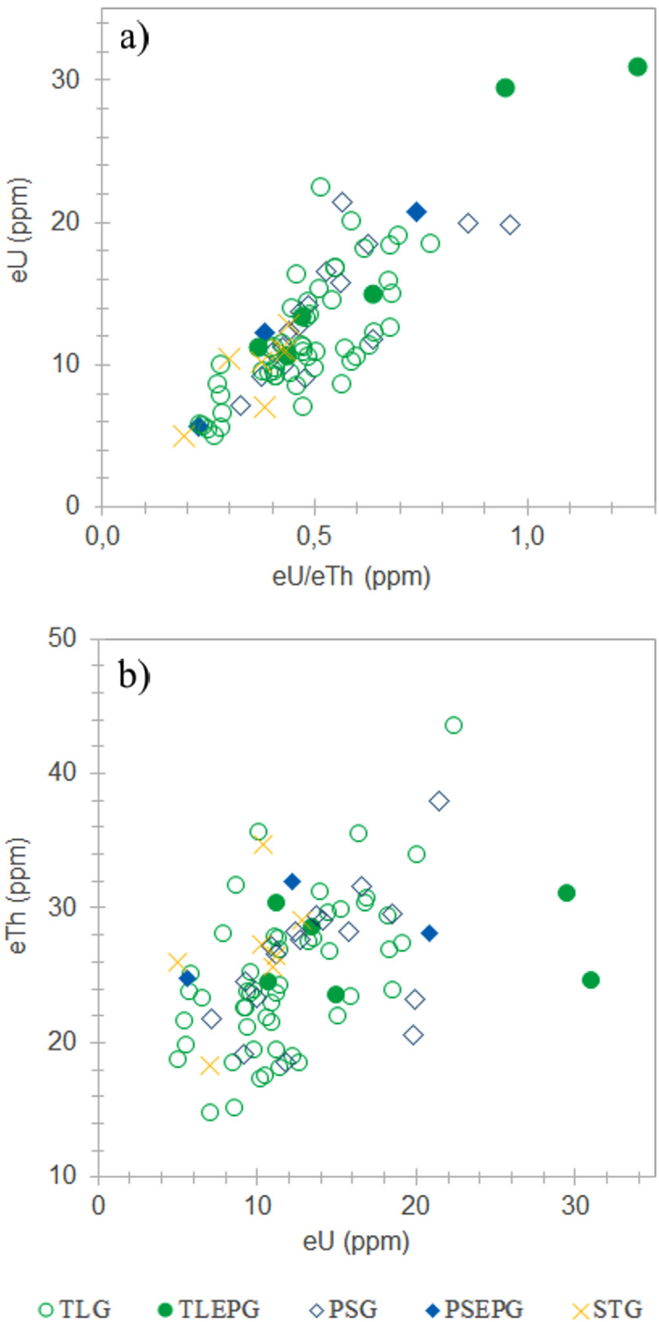

Fig. 4. Variation diagrams for studied biotite granites: a) eU vs. eU/eTh, b) eTh vs. eU.

conditions (Tartèse et al., 2013), it would be important to assess the amount of remobilization of uranium within the plutons, due to those processes. According to Charbonneau (1982) and Heikal et al. (2013), the eU/eTh ratio should remain constant during magmatic fractionation, and any disturbance in this ratio it is indicative either of an enrichment or depletion of uranium. The Fig. 4b shows a positive correlation defined between eU and eU/eTh ratio, suggesting a progressive enrichment of uranium from non-altered granites to some episyenitized granite samples.

According to Jaques et al. (2010), the hydrothermal fluids, directly associated with the episyenitization process of biotite granites from Gerês and Guarda, Portugal, led to magmatic quartz dissolution and transformation of the primary minerals present in granites. Those fluids were trapped in quartz microfractures, and

Table 1
Outdoor and indoor gamma absorbed dose rates with corresponding annual effective dose equivalent rates.

Lithology		Outdoor		Indoor		E (mSv year^{-1})
		D (ηGy h^{-1})	AEDE (μSv year^{-1})	D (ηGy h^{-1})	AEDE (μSv year^{-1})	
TLG	n	51		66		0.93
	Min.	94.9	116.4	94.4	463.1	
	Max.	231.4	283.8	247.5	1214.1	
	Mean	147.8	181.2	163.3	801.1	
TLEPG	n	6		*		
	Min.	170.5	209.1			
	Max.	257.4	315.7			
	Mean	198.2	243.1			
PSG	n	17		18		1.02
	Min.	119.6	146.7	79.7	391.0	
	Max.	223.8	274.5	249.4	1223.5	
	Mean	160.7	197.1	187.2	918.3	
PSEPG	n	3		*		
	Min.	130.5	160.0			
	Max.	190.5	233.6			
	Mean	167.5	205.4			
STG	n	7		2		0.91
	Min.	116.0	142.3	163.8	803.5	
	Max.	170.1	208.6	212.3	1041.5	
	Mean	138.3	169.6	*	*	
Total	Min.	94.9	116.4	79.7	391.0	0.91
	Max.	257.4	315.7	249.4	1223.5	1.02

TLG – Telões granite; TLEPG – Telões episyenite granite; PSG – Pedras Salgadas granite; PSEPG - Pedras Salgadas episyenite granite; STG – Souto granite; n – number of samples; Min. – Minimum; Max. – Maximum;
*Not determined.

are characterised by H_2O-NaCl low-salinity, homogenisation temperatures lower than 300 °C and an alkaline character. Possibly they have a meteoric origin and circulated to a depth lower than 5 km during the final events of the Variscan orogeny. Furthermore, Bobos et al. (2005) and Cabral-Pinto et al. (2014) also suggest that meteoric water warmed by deep circulation through granite faults, shear zones and quartz veins may become enriched in U, P and Mg due to the solubilisation of uranium-bearing minerals, such as thorite, coffinite, and monazite, but also of apatite and chlorite. Uranium from the former solutions could be later adsorbed on Fe oxyhydroxides, weathered surfaces of primary minerals or precipitated at the surface of Fe minerals and apatite (Cabral-Pinto et al., 2014). Therefore, these mechanisms must be considered as potential uranium accumulation processes in comparable areas worldwide.

Outdoor (n=84) and indoor gamma absorbed dose rates (n=86) and corresponding annual effective dose equivalent rates in selected areas of Vila Pouca de Aguiar region are presented in Table 1. The recorded gamma absorbed dose rates for outdoor environments indicates that TLEPG has the highest average (198.2 ηGy h^{-1}), whereas the STG shows the lowest average rate (138.3 ηGy h^{-1}; Table 1). The average rates from indoor measurements range between 163.3 and 188.1 ηGy h^{-1} (Table 1). Thus, considering the standard deviation, there are no significant differences between the average indoor gamma absorbed dose rates, contrary to what would be expected, taking into account the differences in the lithological environment, and the fact of the large majority of the studied rock-built dwellings were made with local granites, because, in general, this is the cheapest solution for the population (Appendix C). The former average values are within the range for outdoor exposure in Portugal 4 to 230 ηGy h^{-1}) and also for indoor exposure 4 to 280 ηGy h^{-1}) (UNSCEAR, 2000). Nevertheless, the maximum values of gamma dose rates for outdoor exposure detected in TLG (231 ηGy h^{-1}) and TLEPG (257 ηGy h^{-1}) exceed those specified in the report of UNSCEAR (2000) (Table 1). The average gamma absorbed dose rates in outdoor and indoor air are much higher than those of the world average (60 ηGy h^{-1}; ICRP, 2004). The annual effective dose rates range from 0.91 mSv y^{-1} in STG to 1.02 mSv y^{-1} in PSG (Table 1). These data are in agreement with a previous study on radioactivity risk of slabs of PSG (Gómez et al., 2011), which indicates that in the worst usage scenario, those slabs yield an estimated annual effective dose of 0.9 mSv y^{-1}. Therefore, the obtained results in this study are comparable with those of Gómez et al. (2011), showing that PSG can be used as a building material, since the dose limit of 1 mSv y^{-1} is not largely exceeded, as recommended by the European Commission (2000).

The geometric mean of radon activity of 91 dwellings from Vila Pouca de Aguiar region is 568 Bq m^{-3}, reaching maximum values of 3432 Bq m^{-3} for TLG, 3906 Bq m^{-3} for contact zones between TLG/PSG, 7066 Bq m^{-3} for PSG and 3046 Bq m^{-3} for STG (Fig. 5a). These values are higher than those obtained in other northern Portuguese granitic areas, namely at Vila Real granite (Gomes et al., 2011) and Amarante granite (Martins et al., 2013), of 364 Bq m^{-3} and 430–220 Bq m^{-3}, respectively. Therefore, in all studied lithologies from Vila Pouca de Aguiar region there is a significant proportion of dwellings (n=57) where the indoor radon average values exceed, by far, the limit defined by the Portuguese legislation regarding the indoor air quality (400 Bq m^{-3}), corresponding to 62.6% of the total (Fig. 5b). However, it must be taken into account that these results are not representative of the annual average since they were collected during the winter, when radon concentrations are usually higher (Neves et al., 2003). The geometric mean of radon activity from dwellings of Vila Pouca de Aguiar show a large variance, which can be mainly attributed to the influence of geogenic factors, such as the local geology. In fact, the presence of geologic faults near dwellings increases their vulnerability to elevated indoor radon by providing favourable pathways from the source uranium-rich bedrock units to the surface (e.g. Drolet and Martel, 2016). However, some architectural characteristics and anthropogenic influences could also explain the observed variability of indoor radon. Therefore, it would be important to mention that dwellings with less than 50 years old (Fig. 6a) and with basement (Fig. 6b) are, in general, better thermally insulated than older dwellings, presenting the highest indoor radon average values, respectively 994 Bq m^{-3} (Fig. 6a) and 1107 Bq m^{-3} (Fig. 6b and Appendix D). Concerning the wall type used in the construction of dwellings, there are no significant differences on indoor radon average values. However, there is a slight tendency to dwellings with walls made of light-weight clay bricks yield the highest values (983 Bq m^{-3}; Fig. 6c and Appendix D). The lack of any kind of passive or active ventilation mechanisms in all studied dwellings with less than 50 years old is probably the main reason to explain this situation. It is also important to mention that dwellings older than 50 years old show construction features that make them really poor thermally insulated, and therefore are “naturally ventilated”. Among the different rooms of dwellings, kitchens and living rooms tend to yield the highest indoor radon average concentrations (898 and 924 Bq m^{-3}, respectively; Fig. 6d and Appendix D), maybe because people tend to kept closed those areas, during winter, in order to avoid heat losses.

The geometric mean of indoor radon concentration in this region (568 Bq m^{-3}; Fig. 5) is also higher than the world's average (40 Bq m^{-3}; UNSCEAR, 2000) and is well above the recommended level of 100 Bq m^{-3} proposed by WHO (2009) and ICRP (2010). The annual effective dose due to indoor radon concentration in the studied area ranges from 17.4 to 40.1 mSv y^{-1} (Table 2). These values are much higher than the world’s average value for the

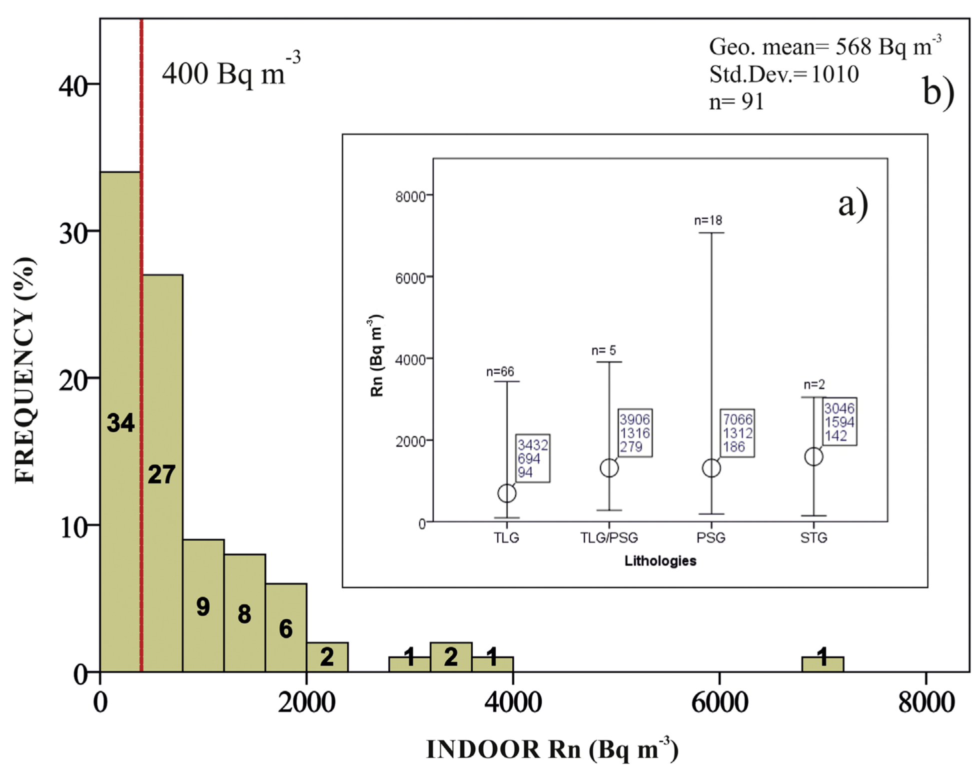

Fig. 5. a) High-low diagrams with average, minimum and maximum of indoor radon for all studied lithologies; b) Indoor radon frequency distribution in the Vila Pouca de Aguiar pluton. The red line corresponds to the indoor radon limit established by Portuguese legislation.

Please cite this article as: Martins, L.M.O., et al., Indoor radon risk associated to post-tectonic biotite granites from Vila Pouca de Aguiar pluton, northern Portugal. Ecotoxicol. Environ. Saf. (2016), http://dx.doi.org/10.1016/j.ecoenv.2016.07.009

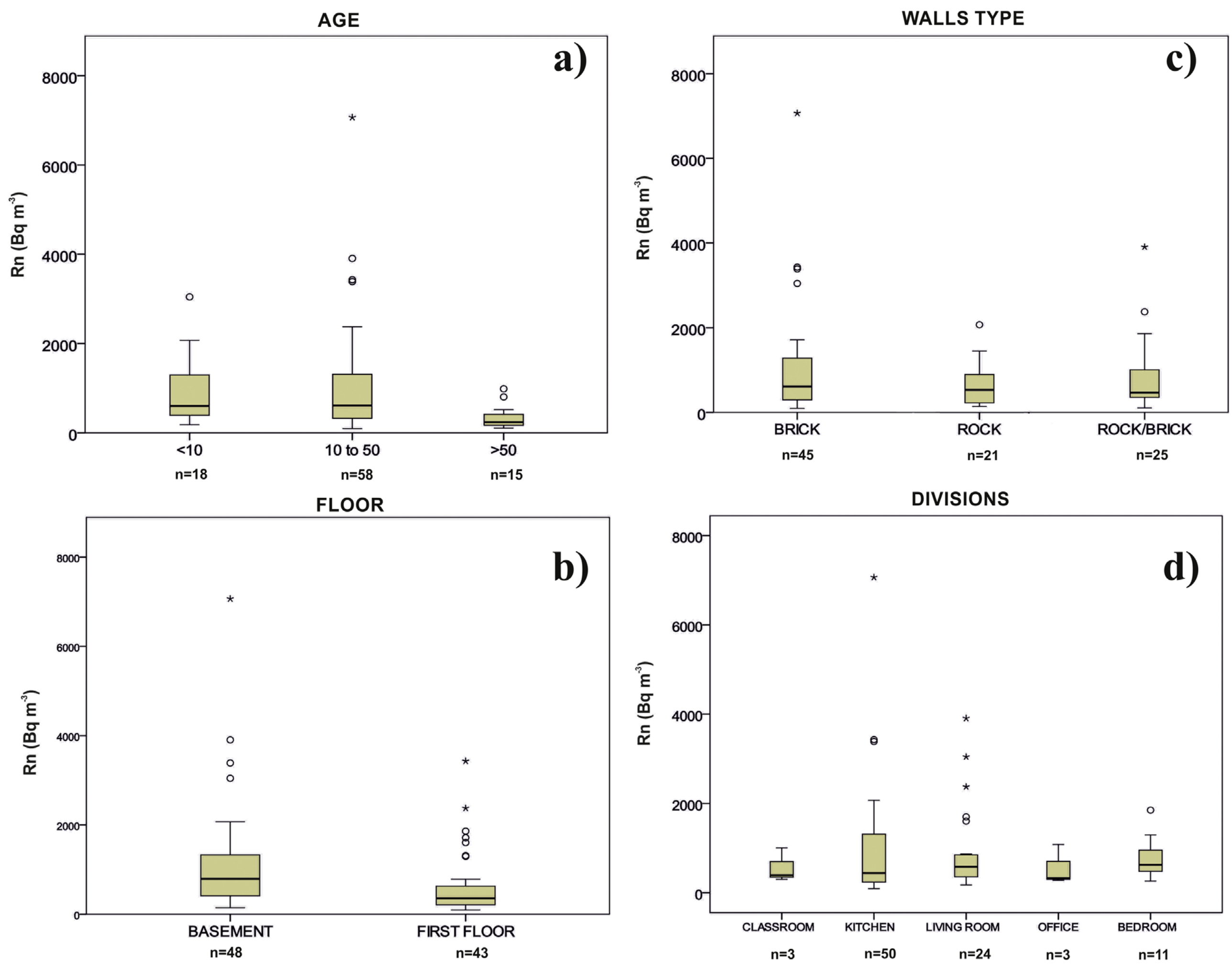

Fig. 6. Boxplot diagrams highlighting the influence of several factors in indoor radon concentrations of Vila Pouca de Aguiar pluton: a) dwellings construction age; b) number of floors in dwellings; c) type of walls used in dwellings construction and d) rooms.

Table 2
Indoor radon concentrations with corresponding annual effective dose equivalent rates (H).

Lithology	Average indoor radon (Bq m^{-3})	H (mSv year^{-1})
TLG	694	17.4
TLG/PSG	1316	33.1
PSG	1312	33.1
STG	1594	40.1

TLG – Telões granite; TLG/PSG – Telões granite in contact with Pedras Salgadas granite; PSG – Pedras Salgadas granite; STG – Souto granite.

inhalation dose due to radon (1.2 mSv y^{-1}), as reported by UNSCEAR (2000). Taking into account that the geometric mean of indoor radon concentration in the Vila Pouca de Aguiar pluton (568 Bq m^{-3}) was just calculated for winter period, the estimated annual mean levels (Bq m^{-3}) of indoor radon concentration were determined based on the criteria establish by Neves et al. (2003), which consider that the increased ventilation of dwellings during the summer provides, in average, a 37% reduction in radon levels in relation to those observed in the winter. Thus, the estimated annual mean of indoor radon for Vila Pouca de Aguiar pluton is 389 Bq m^{-3}, exceeding by far the values presented by Dubois (2005) under the scope of radon survey performed in European countries. In this report the annual mean levels ranges from 19 Bq m^{-3} (Cyprus) to 144 Bq m^{-3} (Serbia-Montenegro).

5. Conclusions

In Vila Pouca de Aguiar pluton, PSG and PSEPG yield the highest average contents of U, whereas STG shows the highest average contents of Th. These results are consistent for non-altered granites, either in field or laboratory radiometric measurements. The enrichment in U is most probably due to the presence of accessory U-bearing minerals such as zircon, while in STG the Th enrichment is probably due to the presence of thorite.

The emplacement of Vila Pouca de Aguiar pluton was controlled by the Régua-Vila Real-Verín fault zone, which crosscuts northern Portugal. In the proximity of faults and joints, TLG and PSG biotite granites are usually affected by different degrees of hydrothermal alteration, forming reddish altered rocks, commonly known as “episyenites”. The late hydrothermal conditions are certainly important in the remobilization of uranium within the plutons, leading to an enrichment of this element in the most advanced stages of episyenitization, such as those observed in some samples of PSEPG, achieving 36 ppm of U.

Concerning external radiation exposure, TLEPG yields the highest average gamma absorbed dose rate, whereas STG shows the lowest average rate. There are no significant differences in the average indoor gamma absorbed dose rates of the different studied granites. However, both average gamma absorbed dose rates in outdoor and indoor air are much higher than those of the world average. The PSG show the highest annual effective dose, but even in the worst usage scenario, it can be used as a building material, since the dose limit of 1 mSv y^{-1}, defined by the European Commission, is not largely exceeded.

The geometric mean of radon activity of 91 dwellings from Vila Pouca de Aguiar region is 568 Bq m^{-3}, being higher than those from other northern Portuguese granitic areas. Therefore, 62.6% of the analysed dwellings, during the winter season, have indoor radon average values, that exceed the limit defined by the Portuguese legislation regarding the indoor air quality (400 Bq m^{-3}). On the other hand, the annual effective dose due to indoor radon concentration in the studied area (17.4–40.1 mSv y^{-1}) are also much higher than the world's average value (1.2 mSv y^{-1}).

The large variance in the geometric mean of radon activity of dwellings from Vila Pouca de Aguiar pluton can be due to the interaction of geogenic, architectural and anthropogenic factors. Among geogenic factors, the role of geologic faults is decisive to increase the indoor radon concentration in dwellings.

This study found evidences that dwellings with less than 50 years old and basement, yield the highest indoor radon average values. Within the sampled dwellings, kitchens and living rooms tend to present the highest indoor radon average concentrations, probably because those areas are preferentially closed by their inhabitants in order to avoid heat losses. Thus, is highly recommended that health authorities start to implement remediation actions in the most severe detected situations. It would be also important to inform the population about the incurred radiological risks to radon exposure and, at the same time, develop awareness campaigns to promote increasing indoor ventilation. Hence, it would be advisable to include radon gas measurement restrictive procedures for licensing new constructions within granitic areas.

Acknowledgements

This study was supported by the Operational Programme and Competitiveness Factors – COMPETE QREN and National Strategic Reference of Foundation for Science and Technology (FCT, Portugal) in the framework of a doctoral fellowship, conceded to Lisa Martins, with SFRH/BD/87336/2012 reference. This research also benefited from some financial support provided by the Centre for Mechanical Engineering, University of Coimbra, Portugal.

Appendix A

See Table A1.

Table A1
Field radiometry data of granites from Vila Pouca de Aguiar pluton.

Lithology	K (%)	eU (ppm)	eTh (ppm)	Lithology	K (%)	eU (ppm)	eTh (ppm)
TLG	6,30	16,83	30,73	**TLEPG**	7,15	31,00	24,63
	6,15	16,73	30,37		6,50	13,43	28,63
	6,65	18,20	29,50		7,44	29,50	31,13
	5,33	11,27	27,73		5,29	14,97	23,53
	4,79	9,73	23,90		7,11	11,20	30,47
	4,21	9,57	23,73		5,97	10,70	24,50
	4,03	12,20	19,07	**n**	6		
	4,11	4,97	18,77	**Min.**	5,29	10,70	23,53
	4,37	10,90	21,57	**Max.**	7,44	31,00	31,13
	4,46	12,57	18,57	**Mean**	6,58	18,47	27,15
	4,99	14,53	26,80	**PSG**	5,93	10,90	27,20
	4,32	11,17	19,47		6,63	18,53	29,57
	4,70	6,57	23,33		5,95	12,40	28,20
	4,51	10,03	35,67		4,44	9,23	24,60
	4,27	9,37	23,87		5,08	12,73	27,60
	4,32	5,40	21,63		4,27	7,10	21,83
	4,43	7,83	28,13		4,85	19,80	20,63
	4,06	9,37	21,17		3,71	9,13	19,13
	4,22	5,53	19,83		4,88	15,80	28,27
	4,77	9,23	22,63		4,93	19,93	23,17
	3,79	9,20	22,57		4,28	11,23	26,57
	4,15	9,77	19,50		6,93	21,43	37,97
	6,02	13,97	31,27		5,03	13,70	29,40
	5,98	16,37	35,63		4,24	9,97	23,30
	8,29	22,40	43,57		5,24	11,80	18,57
	5,28	14,40	29,67		5,40	14,13	29,13
	3,96	15,00	21,97		5,98	16,57	31,57
	4,71	11,20	23,70	**n**	17		
	5,39	19,10	27,37	**Min.**	3,71	7,10	18,57
	6,21	20,07	34,07	**Max.**	6,93	21,43	37,97
	4,07	11,37	24,27	**Mean**	5,16	13,79	26,28
	4,09	5,70	23,83	**PSEPG**	5,83	20,80	28,17
	3,73	8,47	18,53		4,37	5,63	24,83
	4,05	10,20	17,37		5,95	12,20	32,03
	3,81	10,53	17,57	**n**	3		
	4,25	7,00	14,83	**Min.**	4,37	5,63	24,83
	4,60	10,87	23,03	**Max.**	5,95	20,80	32,03
	5,29	15,87	23,47	**Mean**	5,39	12,88	28,34
	4,26	11,40	18,17	**STG**	4,62	10,27	27,30
	4,14	5,80	25,10		4,48	5,03	25,97
	5,35	8,63	31,73		5,04	11,17	26,47
	6,73	8,60	15,20		4,50	11,03	25,57
	5,20	18,33	26,97		5,63	10,40	34,77
	5,72	13,23	27,50		4,12	12,77	29,07
	5,45	15,27	29,93		3,85	7,03	18,33
	4,63	13,53	27,77	**n**	7		
	4,72	11,07	27,93	**Min.**	3,85	5,03	18,33
	5,12	11,43	27,00	**Max.**	5,63	12,77	34,77
	6,95	18,50	23,90	**Mean**	4,61	9,67	26,78
	4,84	9,53	25,30				
	3,77	10,60	21,87				
n	51						
Min.	3,73	4,97	14,83				
Max.	8,29	22,40	43,57				
Mean	4,89	11,75	24,84				

TLG – Telões granite; TLEPG -Telões episyenitized granite; PSG – Pedras Salgadas granite; PSEPG – Pedras Salgadas episyenitized granite; STG – Souto granite; n – number of samples; Min. – Minimum; Max.- Maximum.

Appendix B

See Table B1.

Please cite this article as: Martins, L.M.O., et al., Indoor radon risk associated to post-tectonic biotite granites from Vila Pouca de Aguiar pluton, northern Portugal. Ecotoxicol. Environ. Saf. (2016), http://dx.doi.org/10.1016/j.ecoenv.2016.07.009

Table B1
ORTEC geochemical data of granites from Vila Pouca de Aguiar pluton.

Lithology	K_2O (%)	U (ppm)	Th (ppm)
GTL	5,50	6,70	18,10
	5,00	9,30	19,60
	5,18	9,40	9,80
	4,52	7,30	21,40
n	4		
Min.	4,52	6,70	9,80
Max.	5,50	9,40	21,40
Mean	5,05	8,18	17,23
GTLEP	5,36	4,20	5,80
	5,36	20,90	20,60
	6,19	7,70	24,50
n	3		
Min.	5,36	4,20	5,80
Max.	6,19	20,90	24,50
Mean	5,64	10,93	16,97
GPS	4,92	15,20	22,30
	4,65	14,00	21,40
	4,39	15,80	19,50
n	3		
Min.	4,39	14,00	19,50
Max.	4,92	15,80	22,30
Mean	4,65	15,00	21,07
GPSEP	*	65,50	*
	4,74	6,00	20,20
n	2		
Min.	4,74	6,00	20,20
Max.	4,74	65,50	20,20
GST	5,44	9,00	18,50
	5,57	8,00	26,50
	4,68	15,40	26,60
n	3		
Min.	4,68	8,00	18,50
Max.	5,57	15,40	26,60
Mean	5,23	10,80	23,87

TLG – Telões granite; TLEPG – Telões episyenitized granite; PSG – Pedras Salgadas granite; PSEPG – Pedras Salgadas episyenitized granite; STG – Souto granite; n – number of samples; Min. – Minimum; Max. – Maximum; *Not determined.

Appendix C

See Fig. C1.

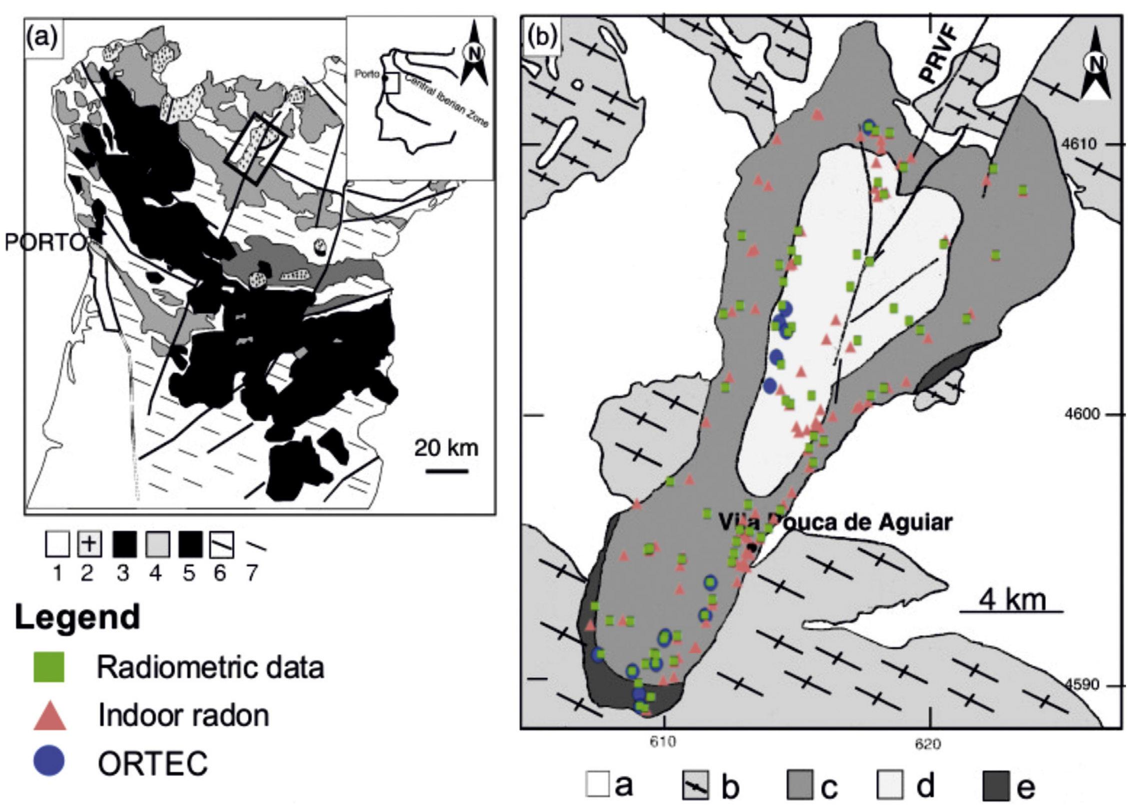

Fig. C1. (a) Geological distribution of Variscan syn- to post-orogenic granitoids in Central Iberian Zone. 1. Post Palaeozoic; 2. Post-orogenic biotite granites; 3. Late-orogenic biotite granites; 4. Synorogenic two-mica granites; 5. Synorogenic biotite granites; 6. Metasedimentary rocks; 7. Faults. (b) Geological map of the Vila Pouca de Aguiar area, with the sampling location. a. Metasedimentary rocks; b. Syntectonic two-mica granite; c. Telões granite (TLG); d. Pedras Salgadas granite (PSG); e. Souto granite (STG). Coordinates: UTM kilometric system; PRVF: Penacova-Régua-Verin Fault; (modified from Martins et al., 2009)

Appendix D

See Table D1.

Table D1
Statistics of features of buildings and associated indoor radon concentration of Vila Pouca de Aguiar region.

Features		Statistic		Std. Error
Age	**< 10**	**Mean**	908	185
		Median	602	
		Std. Dev.	784	
		Minimum	182	
		Maximum	3046	
		n	18	
	10 to 50	**Mean**	994	151
		Median	613	
		Std. Dev.	1150	
		Minimum	94	
		Maximum	7066	
		n	58	
	> 50	**Mean**	347	66
		Median	238	
		Std. Dev.	256	
		Minimum	105	
		Maximum	986	
		n	15	
Floor	**Basement**	**Mean**	1107	171
		Median	792	
		Std. Dev.	1190	
		Minimum	144	
		Maximum	7066	
		n	48	
	First floor	**Mean**	606	104
		Median	354	
		Std. Dev.	683	
		Minimum	94	
		Maximum	3432	
		n	43	
Walls type	**Brick**	**Mean**	983	183
		Median	612	
		Std. Dev.	1226	
		Minimum	94	
		Maximum	7066	
		n	25	
	Rock	**Mean**	646	117
		Median	533	
		Std. Dev.	521	
		Minimum	142	
		Maximum	2072	
		n	21	
	Rock/brick	**Mean**	873	175
		Median	467	
		Std. Dev.	877	
		Minimum	105	
		Maximum	3906	
		n	45	
Divisions	**Classroom**	**Mean**	567	221
		Median	392	
		Std. Dev.	382	
		Minimum	303	
		Maximum	1005	
		n	3	
	Kitchen	**Mean**	898	166
		Median	415	
		Std. Dev.	1173	
		Minimum	94	
		Maximum	7066	
		n	50	
	Living room	**Mean**	924	194
		Median	583	
		Std. Dev.	952	
		Minimum	175	
		Maximum	3906	
		n	24	
	Office	**Mean**	563	261
		Median	325	
		Std. Dev.	452	
		Minimum	279	
		Maximum	1084	
		n	3	
	Bedroom	**Mean**	792	141
		Median	627	
		Std. Dev.	466	
		Minimum	263	
		Maximum	1852	
		n	11	

Std. Error – Standard error; Std. Deviation – Standard deviation; n – number of buildings.

References

Appleton, J., Miles, J., Young, M., 2011. Comparison of Northern Ireland radon maps based on indoor radon measurements and geology with maps derived by predictive modeling of airborne radiometric and ground permeability data, In: Science of the Total Environmental, Elsevier, Vol. 409, pp. 1572–1583.

Appleton, J.D., Miles, J.C.H., 2010. A statistical evaluation of the geogenic controls on indoor radon concentrations and radon risk. J. Environ. Radioact. 101 (10), 799–803.

Baptista, J.C., 1998. Neotectonic study of the area of Penacova-Régua-Verín fault, PhD thesis, UTAD, Vila Real. p. 346.

Basson, I.J., Greenway, G.G., 2004. The rössing uranium deposit: a product of late tectonic localization of uraniferous granites in the central zone of the Damara Orogen, Namibia. J. Afr. Earth Sci. 38, 413–435.

Bobos, I., Jaques, L., Noronha, F., Clauer, N., Liewig, N., 2005. Geochemistry, geothermometry, and K-Ar dating of Episyenitic Rocks associated with the Guarda Uraniferous Granites, ed. Mao, J., Bierlein, F.P., (Eds.), Mineral Deposit Research: Meeting the Global Challenge: Proceedings of the Eighth Biennial SGA Meeting Beijing, China 18–21 August 2005, Vol. I, Springer, pp. 225–228.

Bossew, P., Dubois, G., Tollefsen, T., 2008. Investigations on indoor radon in Austria, part 2: geological classes as categorical external drift for spatial modelling of the radon potential. J. Environ. Radioact. 99, 81–97.

Cabral-Pinto, M.M.S., Silva, M.M.V.G., Neiva, A.M.R., 2014. Release, migration, sorption and (re)precipitation of U during a granite alteration under oxidizing conditions. Procedia Earth Planet. Sci. 8, 28–32.

Cambon A.R., 1994. Uranium deposits in granitic rocks. Notes on the national training course on uranium geology and exploration. Organized by IAEA and NMA, 8–20 Jan 1194, Cairo, Egypt.

Charbonneau B.W., 1982. Radiometric study of three radioactive granites in the Canadian Shield: Elliot Lake, Ontario; Fort Smith, Fury and Hecla, N.W.T. In: Maurice Y.T. (ed) Uranium in granites, Geol. Surv. Canada, pp. 91–99.

Cho, B.-W., Choo, C.O., Kim, M.S., Hwang, J., Yun, U., Lee, S., 2015. Spatial relationships between radon and topographical, geological, and geochemical factors and their relevance in all of South Korea. Environ. Earth Sci. 74 (6), 5155–5168.

Cosma, C., Papp, B., Cucoş-Dinu, A., Sainz, C., 2015. Testing radon mitigation techniques in a pilot house from Băiţa-Ştei radon prone area (Romania). J. Environ. Radioact. 140, 141–147.

Cosma, C., Cucoş-Dinu, A., Papp, Botond, B., Robert, Sainz, C., 2013. Soil and building material as main sources of indoor radon in Băiţa-Ştei radon prone area (Romania). J. Environ. Radioact. 116, 174–179.

Darby, S., Hill, D., Auvinen, A., Barros-Dios, J.M., Baysson, H., Bochicchio, F., Falk, R., Farchi, S., Figueiras, A., Hakama, M., Heid, I., Hunter N., Kreienbrock, L., Kreuzer, M., Lagarde, F., Mäkeläinen, I., Muirhead, C., Oberaigner, W., Pershagen, G., Ruosteenoja, E., Scaffrath, A. R., Tirmarche, M., Tomášek, L., Whitley, E., Wichmann, H.E., Doll, R., 2005. Radon in Homes and Risk of Lung Cancer: Collaborative Analysis of Individual Data From 13 European case–control studies. BMJ; 330, January ,7485, 223.

Decree-Law nr. 79/2006, 4 of April, Indoor air quality, Journal of the Portuguese Republic, Series I no. 67, Ministry of Public Works, Transport and Communications.

Dezayes, C., Genter A., Hooijkaas G.R., 2005. Deep-seated geology and fracture system of the EGS Soultz reservoir (France) based on Recent 5 km Depth Boreholes, In: Proceedings World Geothermal Congress 2005 Antalya, Turkey, 24–29.

Drolet, J.-P., Martel, R., 2016. Distance to faults as a proxy for radon gas concentration in dwellings. J. Environ. Radioact. 152, 8–15.

Dubois G., 2005. An overview of radon surveys, In: Radioactivity Environmental Monitoring Emissions And Health Unit Institute For Environment And Sustainability JRC-European Commission, EUR 21892 EN, EC, Europe, 168.

European Commission, 2000. Radiation Protection 112 Radiological Protection Principles Concerning the Natural Radioactivity of Building Materials, Office for official publications of the European Communities, Luxembourg.

Friedmann, H., Groeller, J., 2010. An approach to improve the Austrian radon potential map by Bayesian statistics. J. Environ. Radioact. 101, 804–808.

Genter, A., Traineau, H., 1992. Borehole EPS-1. Drilling, V 3. Preliminary Geological

Results From Granite Core Analyses For Hot Dry Rock Research. Scientific,, Alsace, France, pp. 205–214.
Genter, A., Dezayes, Ch., Gentier, S., Ledesert, B. and Sausse, J., 2002. Conceptual fracture model at Soultz based on geological data, In: Editors Baria, R., Baumgärtner, J., Gérard, A., Reinhard, J., Geologishes Jahrbuch, International Conference 4th HDR Forum, Strasbourg, France, 1998:93–102.
Girault, F., Perrier, F., 2012. Estimating the importance of factors influencing the radon-222 flux from building walls. Sci. Total Environ. 433, 247–263.
Gomes, M.E.P., 2008. Geochemistry of microgranular enclaves and host granite from Telões (Vila Pouca de Aguiar), Northern Portugal. Chem. Erde Geochem. 68, 69–80.
Gomes, M.E.P., Neves, L.J.P.F., Coelho, F., Carvalho, A., Sousa, M., Pereira, A.J.S.C., 2011. Geochemistry of granites and metasediments of the urban area of Vila Real (northern Portugal) and correlative radon risk. Environ. Earth Sci. 64 (2), 497–502.
Gómez, D., Neves, L., Pereira, A., Neila, C., 2011. Natural radioactivity in ornamental stones: an approach to its study using stones from Iberia. Bull. Eng. Geol. Environ. 70 (4), 543–547.
Groves-Kirkby, C.J., Crockett, R.G.M., Denman, A.R., Phillips, P.S., 2015. A critical analysis of climatic influences on indoor radon concentrations: implications for seasonal correction. J. Environ. Radioact. 148, 16–26.
Groves-Kirkby, C.J., Denman, A.R., Crockett, R.G.M., Phillips, P.S., Gillmore, G.K., 2006. Identification of tidal and climatic influences within domestic radon time-series from Northamptonshire, UK. Sci. Total Environ. 367 (1), 191–202.
Heikal, M.T.S., El-Dosuky, B.T., Ghoneim, M.F., Sherif, M.I., 2013. Natural radioactivity in basement rocks and stream sediments, Sharm El Sheikh Area, South Sinai, Egypt: Radiometric Levels and their Significant Contributions, Arabian Journal of Geosciences, 6, 9, pp. 3229–3239.
ICRP, 2004. Development of the Draft 2005 Recommendations of the ICRP – A Collection of Papers, ICRP Supporting Guidance 4 Ann. ICRP, 34(S), 2004.
ICRP, 2010. Lung Cancer Risk from Radon and Progeny and Statement on Radon – ICRP Publication 115 Annals of the ICRP, Vol. 40, pp. 1–64.
Ielsch, G., Cushing, M.E., Combes, P., Cuney, M., 2010. Mapping of the geogenic radon potential in France to improve radon risk management: methodology and first application to region Bourgogne. J. Environ. Radioact. 101, 813–820.
Janik, M., Omorib, Y., Yonehara, H., 2015. Influence of humidity on radon and thoron exhalation rates from building materials. Appl. Radiat. Isot. 95, 102–107.
Jaques, L., Bobos, I., Noronha, F., 2010. Study of fluids related to hydrothermal alteration of biotite granites from Gerês and Guarda (Portugal). Geol. Commun. 97, 81–98.
Kemski, J., Klingel, R., Siehl, A., Valdivia-Manchego, M., 2009. From radon hazard to risk prediction-based on geological maps, soil gas and indoor measurements in Germany. Environ. Geol. 56, 1269–1279.
Kobayashi, T., 2000. Concentration ratio of radon progeny in air, In: Proceedings of the 10th International Congress of the International Radiation Protection Association, Hiroshima, Japan, May 14 e 19, 2000.
Kropat, G., Bochud, F., Jaboyedoff, M., Laedermann, J.-P., Murith, C., Palacios, M., Baechler, S., 2014. Major influencing factors of indoor radon concentrations in Switzerland. J. Environ. Radioact. 129, 7–22.
Lamas, R., Miranda, M., Neves, L., Pereira. A., 2015. Radiogenic heat production from a deep borehole in the Beiras granite (Almeida, Central Portugal), In: Proceedings of Conference in Energy for Sustainability 2015, Sustainable cities: Designing for people and the planet, 14–15 May, Coimbra, Portugal.
Martins, H., Sant'Ovaia, H., Noronha, F., 2009. Genesis and emplacement of felsic Variscan plutons within a deep crustal lineation, the Penacova-Régua-Verín fault: an integrated geophysics and geochemical study (NW Iberian Peninsula). Lithos 111 (3–4), 142–155.
Martins, L.M.O., Gomes, Maria, E.P., Neves, L.J.P.F., Pereira, A.J.S.C., 2013. The influence of geological factors on radon risk in groundwater and dwellings in the region of Amarante (Northern Portugal). Environ. Earth Sci. 68 (3), 733–740.
Miles, J.C.H., 2001. Temporal variation of radon levels in houses and implications for radon measurement strategies. Radiation Protection Dosimetry, 93, pp. 369–376.
Neves, L.J.P.F, Avelans, S.C.C., Pereira, A.J.S.C., 2003. Seasonal variation radon gas in dwellings in the urban area of the Guarda (Central Portugal), In: Proceedings of the IV Iberian Congress of Geochemistry, XIII Week Geochemistry, Coimbra, Portugal, pp. 307–309.
Pereira, A.J.S.C., Godinho, M.M., Neves, L.J.P.F., 2010. On the influence of faulting on small-scale soil-gas radon variability: a case study in the Iberian Uranium Province. J. Environ. Radioact. 101 (10), 875–882.
Perrier, F., Richon, P., Sabroux, J.C., 2009. Temporal variations of radon concentration in the saturated soil of Alpine grassland: the role of groundwater flow. Sci. Total Environ. 407, 2361–2371.
Perrier, F., Girault, F., 2013. Harmonic response of soil radon-222 flux and concentration induced by barometric oscillations. Geophys. J. Int. 195, 945–971.
Ribeiro, M.A., 1998. Lithogeochemistry Study of Metasedimentary Rocks Formations and Mineralizations in Tras-os-Montes West, Metallogenic implications. PhD thesis, Oporto University, 231p.
Sant'Ovaia H., Bouchez, J.L., Noronha, F., Leblanc, D., Vigneresse, J.L., 2000. Composite-laccolith emplacement of the post-tectonic Vila Pouca de Aguiar granite pluton (northern Portugal): a combined MAS and gravity study. Trans. R. Soc. Edinb.: Earth Sci.: Earth Sci. 91, 123–137.
Tartèse, R., Boulvais, P., Poujol, M., Gloaguen, E., Cuney, M., 2013. Uranium mobilization from the variscan questembert syntectonic granite during fluid-rock interaction at depth. Econ. Geol. 108 (2), 379–386.
UNSCEAR, 2008. Sources and Effects of Ionizing Radiation, United Nations, New York, p. 472.
UNSCEAR, 2000. REPORT Vol. I Sources and Effects of Ionizing Radiation, Annex A: Dose Assessment Methodologies. United Nations Scientific Committee on the Effects of Atomic Radiation: New York.
Veloso, B., Nogueira, J., Cardoso, M.F., 2012. Lung cancer and indoor radon exposure in the north of Portugal-an ecological study. Cancer Epidemiol. 36 (1), e26–e32.
WHO, 2009. World health organization (Vol. I) In: Shannoun HZa, (ed.) WHO Handbook on Indoor Radon, A Public Health Perspective, Geneva, Switzerland.
Wilson, M.R., ÅKERBLOM, G.V., 1982. Geological setting and geochemistry of uranium rich granites in the Proterozoic of Sweden. Mineral. Mag. 46, 233-45.

Please cite this article as: Martins, L.M.O., et al., Indoor radon risk associated to post-tectonic biotite granites from Vila Pouca de Aguiar pluton, northern Portugal. Ecotoxicol. Environ. Saf. (2016), http://dx.doi.org/10.1016/j.ecoenv.2016.07.009